Initial results of high-latitude magnetopause and low-latitude flank flux transfer events from 3 years of Cluster observations

Y. L. Wang,[1] R. C. Elphic,[1] B. Lavraud,[1] M. G. G. T. Taylor,[1,2] J. Birn,[1] J. Raeder,[3] C. T. Russell,[4] H. Kawano,[5] Q.-G. Zong,[6] H. Zhang,[6] X. X. Zhang,[7] and R. H. Friedel[1]

Received 24 March 2005; revised 5 July 2005; accepted 1 September 2005; published 26 November 2005.

[1] We present initial results from a statistical study of Cluster multispacecraft flux transfer event (FTE) observations at the high-latitude magnetopause and low-latitude flanks from February 2001 to June 2003. Cluster FTEs are observed at both the high-latitude magnetopause and low-latitude flanks for both southward and northward IMF. Among the 1222 FTEs, 36%, 20%, 14%, and 30% are seen by one, two, three, and four Cluster satellites, respectively. There are 73% (27%) of the FTEs observed outside (inside) the magnetopause, which might be caused by the motion of FTEs toward the magnetosheath when they propagate from subsolar magnetopause to the midlatitude and high-latitude magnetopause and low-latitude flanks. We obtain an average FTE separation time of 7.09 min, which is at the lower end of the previous results. The mean B_N peak-peak magnitude of Cluster FTEs is significantly larger than that from low-latitude FTE studies. FTE B_N peak-peak magnitude clearly increases with increasing absolute magnetic latitude (MLAT), it has a weaker dependence on magnetic local time (MLT) with a peak near the magnetic local noon, and it has a complex dependence on Earth dipole tilt with a peak at around zero. FTE periodic behavior is found to be controlled by MLT, with a general increase of FTE separation time with increasing MLT, and by Earth dipole tilt, with a peak FTE separation time at around zero Earth dipole tilt. There is no clear dependence of FTE separation time on MLAT. There is a weak increase of FTE B_N peak-peak magnitude with increasing FTE separation time, and we see no clear dependence of it on FTE B_N peak-peak time. When no FTE identification thresholds are used, more accurate calculations of some FTE statistical parameters, including the mean B_N peak-peak time, can be obtained. Further, comparing results with different thresholds can help obtain useful information about FTEs.

Citation: Wang, Y., et al. (2005), Initial results of high-latitude magnetopause and low-latitude flank flux transfer events from 3 years of Cluster observations, *J. Geophys. Res.*, *110*, A11221, doi:10.1029/2005JA011150.

1. Introduction

[2] Flux transfer events (FTEs) are believed to be the results of temporally and spatially varying, i.e., patchy and impulsive, magnetic reconnection at the magnetopause. It has been shown from observations that FTEs contain a mixture of magnetospheric and magnetosheath plasmas [e.g., *Daly et al.*, 1981; *Paschmann et al.*, 1982; *Saflekos et al.*, 1990; *Le et al.*, 1993]. Thus they are important for the coupling of mass, momentum, and energy between the solar wind and the Earth's magnetosphere. Since the discovery of FTEs [*Russell and Elphic*, 1978, 1979; *Haerendel et al.*, 1978], their statistical properties have been widely studied [e.g., *Paschmann et al.*, 1982; *Berchem and Russell*, 1984; *Rijnbeek et al.*, 1984; *Southwood et al.*, 1986; *Elphic*, 1990; *Kawano et al.*, 1992; *Kuo et al.*, 1995; *Kawano and Russell*, 1996, 1997a; *Sanny et al.*, 1996, 1998]. In addition to the original flux rope model proposed by *Russell and Elphic* [1978], several other FTE models have been proposed to explain the FTE formation based on large-scale FTE statistical results [e.g., *Lee and Fu*, 1985; *Scholer*, 1988; *Sibeck*, 1990; *Liu et al.*, 1992].

[3] FTE separation time and B_N peak-peak magnitude provide important information about the generation mechanism and dynamics of FTEs. *Rijnbeek et al.* [1984] studied ISEE observations and found a mean FTE separation time of ~7–8 min. *Lockwood and Wild* [1993] also studied ISEE

[1]Space Science and Applications, Los Alamos National Laboratory, Los Alamos, New Mexico, USA.
[2]Mullard Space Science Laboratory, University College London, London, UK.
[3]Space Science Center, University of New Hampshire, Durham, New Hampshire, USA.
[4]Institute of Geophysics and Planetary Physics, University of California, Los Angeles, Los Angeles, California, USA.
[5]Department of Earth and Planetary Sciences, Kyushu University, Fukuoka, Japan.
[6]Center for Space Physics, Boston University, Boston, Massachusetts, USA.
[7]Key Laboratory of Space Weather, Center for Space Science and Applied Research, Beijing, China.

0148-0227/05/2005JA011150$09.00

observations and found a mean time interval between two FTEs of 8 min. *Kuo et al.* [1995] obtained 10.5 min (median: 8 min) FTE separation time from their ISEE 1 FTE study. *Neudegg et al.* [2000] found from their Equator-S FTE observations an average FTE separation time of 8.8 min, assuming intervals larger than 20 min are not part of the same reconnection sequence. *Kawano and Russell* [1996] developed an automatic program to identify FTEs and surveyed 9 years of ISEE 1 observations. They found a median B_N peak-peak magnitude of 14 nT and a median B_N peak-peak duration of 36 s. They believed that these values are upper estimates because the automatic algorithm used in their study rejects events with small B_N peak-peak magnitude and duration. In contrast, *Sanny et al.* [1996] obtained a median B_N peak-peak duration time of 3 min, much larger than *Kawano and Russell*'s [1996] result.

[4] FTE structures inside and outside of the magnetopause have been found to be the same physical phenomenon [*Rijnbeek et al.*, 1984; *Kuo et al.*, 1995]. *Neudegg et al.* [2000] found that 75% of their 87 midlatitude FTEs are in the magnetosheath, while the rest are in the magnetosphere or on the magnetopause. In contrast, *Rijnbeek et al.* [1984], *Berchem and Russell* [1984], and *Kawano and Russell* [1996] from their low-latitude ISEE 1 and 2 observations found FTE signatures with nearly equal frequency inside and outside of the magnetopause.

[5] *Russell et al.* [1997] studied flux transfer events occurred at times of steady IMF and found that FTE quasi-periodic behavior is controlled by the magnetopause or the magnetosphere and is not driven by the external boundary conditions. However, few dedicated studies so far have been conducted to investigate the relation between FTE periodic behavior and magnetopause/magnetosphere properties.

[6] Although these previous FTE statistical studies have provided important information about FTEs, most of them concentrated on low-latitude and midlatitude magnetopause observations and ground observations. There has been a scarcity in studies examining the statistical properties of high-latitude FTEs, possibly due to the complication of the vicinity of the cusp. Cluster observations provide a great opportunity to advance the understand of FTEs in this region, not only because Cluster has a trajectory which encounters the high-latitude magnetopause but also because Cluster consists of four spacecraft allowing detailed study of FTE structure and motion. Cluster FTE-related event studies have already been conducted by some authors [e.g., *Wild et al.*, 2001; *Owen et al.*, 2001; *Bosqued et al.*, 2001; *Zong et al.*, 2003; *Vontrat-Reberac et al.*, 2003; *Sonnerup et al.*, 2004; *Thompson et al.*, 2004]. Most recently, Y. L. Wang et al. (The dependence of flux transfer events on geophysical parameters from three years of cluster observations, submitted to *Annales Geophysicae*, 2005, hereinafter referred to as Wang et al., submitted manuscript, 2005) reported Cluster FTE dependence on geophysical parameters: MLT, MLAT, and Earth dipole tilt. They found that in the normalized FTE MLT distribution, more FTEs are observed from dawn to dusk from $\sim$9 to $\sim$17 MLT. Also, they found that FTE occurrence is reduced when the dipole tilt is close to zero. Also, when dipole tilt is positive (negative), Cluster observes more FTEs in the southern (northern) hemisphere. This Cluster FTE Earth dipole tilt dependence is consistent with the FTE global model simulation results by *Raeder* [2005].

[7] The purpose of this paper is to extend the study by Wang et al. (submitted manuscript, 2005) and make use of the large Cluster FTE data set to have a detailed study of some important properties of Cluster high-latitude magnetopause and low-latitude flank FTEs. In the paper we first have a detailed discussion of the stretched *Shue et al.* [1998] magnetopause model for Cluster magnetic field LMN coordinate transformation. Then, we give a brief introduction to the instrumentation and data used in this study, including our criteria for FTE identification. In section 4 we show the results of this FTE statistical study. Finally, we discuss and summarize our findings.

2. Stretched *Shue et al.* [1998] Magnetopause Model

[8] FTE signatures have proven to show best in the LMN boundary coordinate system [*Russell and Elphic*, 1978]. In this system the magnetic field can be decomposed as B_N along the outward normal to the magnetopause, B_L along the projection of the Earth dipole axis onto the magnetopause (positive northward), and B_M directed dawnward. A convenient way to construct an LMN coordinate system is through a magnetopause model. The empirical magnetopause model of *Shue et al.* [1998] has been shown to be one of the magnetopause models with smallest errors [*Suvorova et al.*, 1999]. In this model, an analytical form of the magnetopause location is used to best fit magnetopause location observations:

$$r = r_0 \left(\frac{2}{1 + \cos\theta} \right)^{\alpha}, \qquad (1)$$

where

$$r_0 = \{10.22 + 1.29 \tanh[0.184(B_z + 8.14)]\} P_{dyn}^{-1.0/6.6},$$

$$\alpha = (0.58 - 0.007 B_z)\left[1 + 0.024 \ln P_{dyn}\right].$$

Here B_z is the IMF z component in nT in GSM coordinates, P_{dyn} is the solar wind dynamic pressure in nPa, and θ is the angle between the Earth-Sun line and magnetopause location vector, $\mathbf{r}$.

[9] In practice, the spacecraft magnetopause crossing location, ($\boldsymbol{r}'$, θ'), is very likely to be away from the model magnetopause surface. Such an inconsistency may lead to errors in the LMN transformation. To solve this problem, we stretch the *Shue et al.* [1998] magnetopause model radially, with the same ratio for each Cluster magnetopause crossing, to fit each spacecraft crossing location. This leads to

$$r = r' \left(\frac{1 + \cos\theta'}{1 + \cos\theta} \right)^{\alpha}. \qquad (2)$$

In this study we use this method for each magnetopause crossing to perform the LMN transformation.

3. Instrumentation and Data

[10] The Cluster mission was launched in 2000, and it consists of four identical satellites. Cluster's orbit has a 90° inclination with a perigee of 4 R_E and an apogee of 19.6 R_E. The plane of Cluster's orbit precesses clockwise looking down from the north, and it extends outside of the magnetopause from near the end of one year to

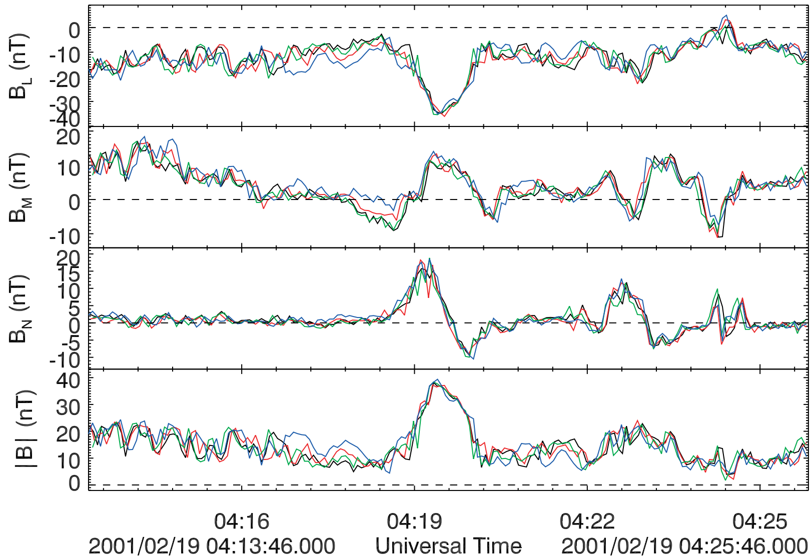

Figure 1. A sample Cluster FTE observed at ~0420 UT on 19 February 2001 at (5.8, 0.8, 10.2) R_E in GSM coordinates. Different line colors stand for different Cluster satellites. This FTE shows clear B_N bipolar signature and $|\mathbf{B}|$ enhancement. Note here that there is also a less clear FTE at ~0423 UT.

around July of the next year, during which FTEs can be observed. In this study, we surveyed the first 3 years of Cluster FTE observations from February 2001 to June 2003. Cluster magnetic field observations from the Fluxgate Magnetometer (FGM) [*Balogh et al.*, 1997] and plasma observations from the Cluster Ion Spectrometry (CIS) instrument [*Rème et al.*, 2001] were used to identify Cluster magnetopause crossings, and FGM observations were used for FTE identifications. We use ACE Solar Wind Electron Proton Alpha Monitor (SWEPAM) [*McComas et al.*, 1998] and Magnetic Field Instrument (MFI) [*Smith et al.*, 1998] observations for the stretched [*Shue et al.*, 1998] magnetopause model calculations and IMF sorting of the FTEs. The time shift of the ACE observations for each FTE is visually determined by matching Cluster magnetosheath magnetic field clock angles and ACE IMF clock angles close to the Cluster magnetopause crossing related to this FTE.

[11] Previous studies have used numerous criteria to identify FTEs, most commonly adopted is a B_N bipolar signature and $|\mathbf{B}|$ enhancement [*Russell and Elphic*, 1978]. *Rijnbeek et al.* [1984] used a much more relaxed version of the above pattern criteria which does not require obvious $|\mathbf{B}|$ enhancement. *Berchem and Russell* [1984] used B_N bipolar signature and $|\mathbf{B}|$ enhancement, but they also included the tangential field increase and rotation toward a direction that lies neither along the magnetosheath nor along the magnetospheric field orientations. However, *Paschmann et al.* [1982] found from ISEE 1 and 2 observations that the B_L and B_M components showed considerable variation from event to event. In addition, *Kawano and Russell* [1996] showed that there were only 933 out of their 1246 FTEs showing rotational polarity in the MN plane. In our present study we inspect Cluster magnetic field time series data to isolate FTEs such that they show clear B_N bipolar signature and $|\mathbf{B}|$ enhancement. We also require that an FTE clearly isolates itself from its surroundings, which avoids identifying FTEs in highly oscillating field structures. A sample Cluster FTE fitting such criteria was observed at ~0420 UT on 19 February 2001 at (5.8, 0.8, 10.2) R_E in GSM coordinates and its magnetic field observations are shown in Figure 1.

[12] Many quantitative FTE identification thresholds have also been used in previous studies, for example, minimum B_N peak-peak magnitude and minimum FTE duration [e.g., *Rijnbeek et al.*, 1984; *Southwood et al.*, 1986; *Kuo et al.*, 1995; *Kawano and Russell*, 1996]. During our visual identification of Cluster FTEs, we did not apply any such thresholds because some clear FTE signatures do not fit the arbitrary thresholds used by some previous studies. Note here that there is still an actual lower limit of B_N peak-peak time of 4 s in this study because of the Cluster data sampling rate. Here B_N peak-peak time is defined as the time between B_N positive and negative peaks in each FTE. In this way, we can keep as many events with as large spatial and temporal scales as possible. *Southwood et al.* [1986] pointed out in their UKS spacecraft FTE study that their use of an amplitude threshold criterion in event selection was solely for operational purposes, and it is entirely possible that there is a continuous graduation in scale of events. Also, they believed that the different criteria used in the FTE studies should not influence the results in a significant way. Wang et al. (submitted manuscript, 2005) found from their Cluster FTE study that different FTE selection thresholds change some, but not all, statistical results in a significant way. They believed that the case that different thresholds caused big differences was the result of Cluster orbital bias. To obtain more profound understanding about the influence of FTE criteria on FTE statistical results, we make more investigations using the same criteria as used by Wang et al. (submitted manuscript, 2005): $|B_{N,peak-peak}| \geq 10$ nT and $|\mathbf{B}|_{peak-surrounding} \geq 10$ nT (Threshold 1); $|B_{N,peak-peak}| \geq 17$ nT and $|\mathbf{B}|_{peak-surrounding} \geq 17$ nT (Threshold 2). For convenience, we define Threshold 0 as the case without thresholds.

4. Results

[13] From February 2001 to June 2003, 1222 FTEs are identified using the visual criteria discussed in section 3

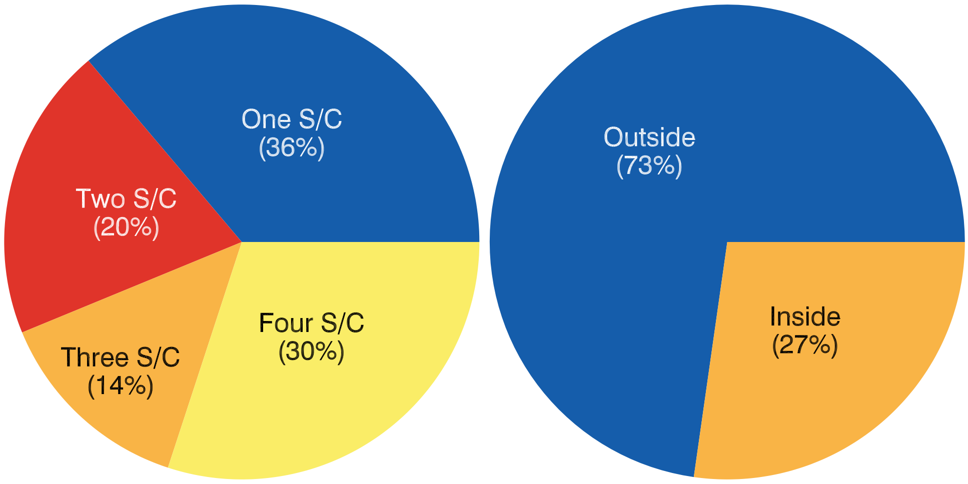

Figure 2. The left panel shows the percentages of the number of Cluster spacecraft seeing the same FTEs, and the right panel shows the percentages of the FTEs inside and outside of the magnetopause, all without thresholds.

without quantitative FTE identification thresholds (Threshold 0). The left panel of Figure 2 shows the percentages of the number of Cluster spacecraft seeing the same FTEs without thresholds. Because FTEs have limited sizes in space and Cluster satellites are separated from each other, sometimes only a few, but not all, Cluster satellites see the same FTEs. In 36%, 20%, 14%, and 30% of the 1222 FTEs, one, two, three, and four Cluster satellites see the same FTEs, respectively. If an FTE is seen by multiple Cluster satellites, we choose the FTE observations from the Cluster satellite with the best FTE signatures for the statistics later in the paper. Why some FTEs are observed by all the four satellites, while some else are observed by only one, should be related to the relative distance of the four satellites, which is a topic of future research. The right panel of Figure 2 shows the percentages of the FTEs inside and outside of the magnetopause for the case without thresholds. There are 73% (27%) of the FTEs observed outside (inside) the magnetopause. Note here that the FTEs inside the magnetopause crossings are not necessarily in the magnetosphere. Instead, they may also be in the cusp region. Further study shows that the percentages of FTEs inside/outside of the magnetopause do not change much for low-latitude and high-latitude FTEs: for low-latitude FTEs ($|z_{gsm}| < 7.5\ R_E$), 69% (31%) FTEs are observed outside (inside) the magnetopause; for high-latitude FTEs ($|z_{gsm}| > 7.5\ R_E$), 76% (24%) FTEs are observed outside (inside) the magnetopause.

[14] Figure 3, from top to bottom, shows the locations of the FTEs without thresholds in the GSM *xz*, *yz*, and *xy* planes, respectively; from left to right, shows the FTEs during all, southward, and northward IMF orientations, respectively. Tsyganenko 1996 magnetic field model [*Tsyganenko*, 1995] field lines are shown as the background in each panel for reference. From the figure, we see that many of the FTEs are observed at the high-latitude magnetopause near the cusps. However, there are also a considerable number of low-latitude FTEs near the magnetopause flanks. In the middle and right panels of Figure 3, FTEs are observed at both the high-latitude magnetopause and low-latitude flanks for both southward and northward IMF conditions.

[15] Figure 4 shows the FTE separation time distribution, FTE $|\mathbf{B}|_{peak-surrounding}$ distribution, FTE B_N peak-peak time distribution, and FTE B_N peak-peak magnitude distribution, all with no thresholds. Note here that each FTE separation time in the upper left panel is calculated between two contiguous FTEs without requiring that they correspond to the same Cluster magnetopause crossing. From the figure, we see that all these distributions show more or less smooth profiles. The mean FTE separation time is 37.15 min (median: 12.12 min), the mean FTE $|\mathbf{B}|_{peak-surrounding}$ is 13.13 nT (median: 11.07 nT), the mean B_N peak-peak time is 25.80 s (median: 20.07 s), and the mean B_N peak-peak magnitude is 25.36 nT (median: 22.09 nT).

[16] Table 1 shows some FTE statistical parameters for Thresholds 0, 1, and 2. As pointed out by Wang et al. (submitted manuscript, 2005), with tighter thresholds, a larger proportion of FTEs are seen during southward IMF (57% for Threshold 0, 61% for Threshold 1, and 65% for Threshold 2). Although the proportion of northward IMF FTEs decreases with increasing threshold, the occurrence rate stays relatively high even for very tight threshold conditions. It is unlikely that such constraints result in the selection of phenomena other than FTEs. Therefore the large occurrence rate during northward IMF FTEs is realistic. Also seen in the table is that the mean B_N peak-peak time has little dependence on thresholds, similar to the portion of the FTEs seen inside and outside of the magnetopause. Because of the increasing $|B_{N,peak-peak}|$ and $|\mathbf{B}|_{peak-surrounding}$ thresholds from Threshold 0 to Threshold 2, we see increase in the mean $|B_{N,peak-peak}|$ and $|\mathbf{B}|_{peak-surrounding}$ as expected.

[17] Figure 5, from left to right, shows the FTE B_N peak-peak magnitude dependence on MLT, MLAT, and Earth dipole tilt, all without quantitative FTE identification thresholds. The thick horizontal bars are the medians of FTE B_N peak-peak magnitude for the MLT, MLAT, and Earth dipole tilt ranges that they span. The thin horizontal bars are the standard errors of the median values that they correspond. In Figure 5, there is a weak dependence of FTE B_N peak-peak magnitude on MLT with a peak near 12 MLT and the magnitude generally decreases farther away from the magnetic local noon. In contrast, FTE B_N peak-peak

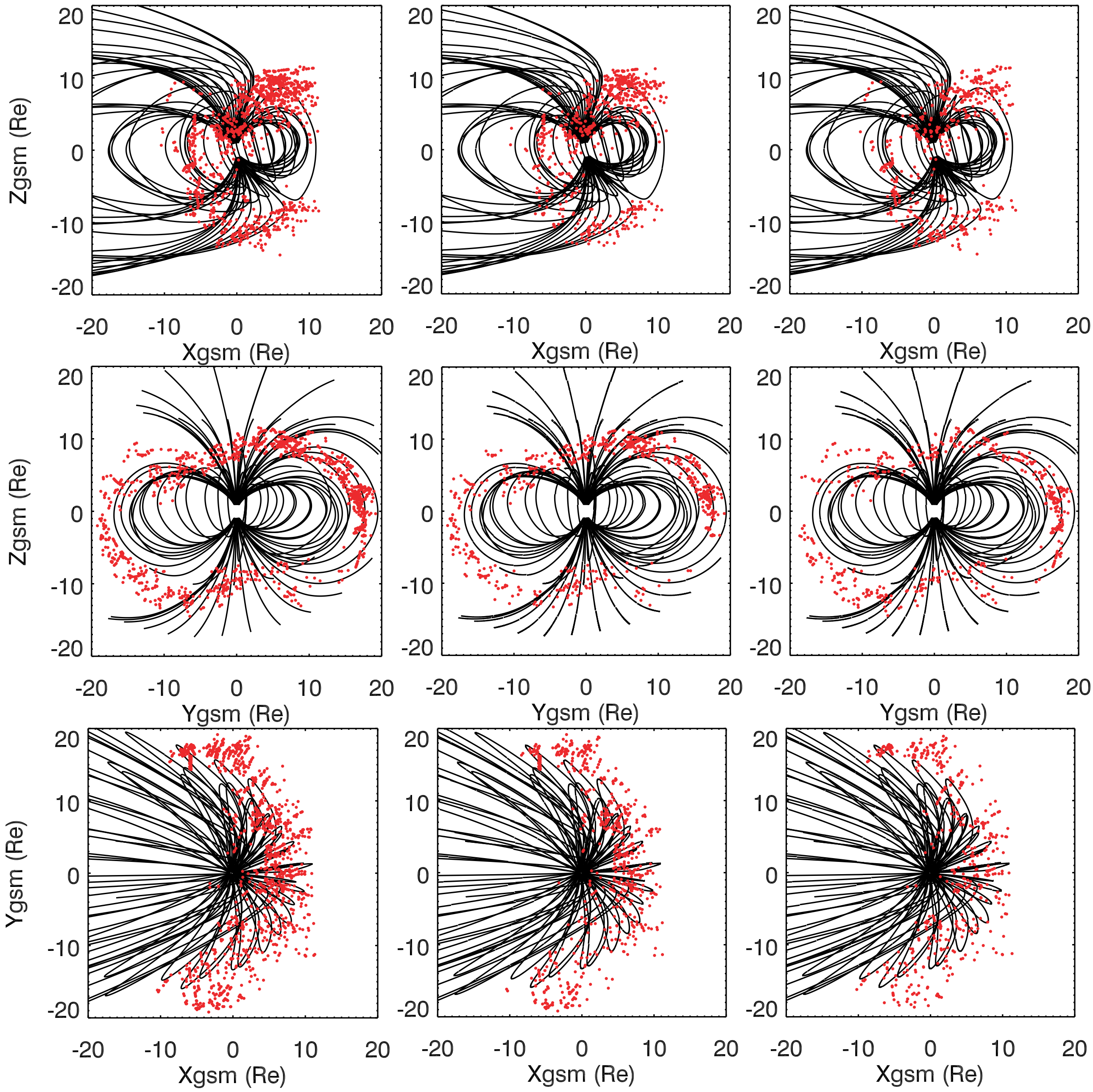

Figure 3. From top to bottom: The locations of the FTEs in the GSM *xz*, *yz*, and *xy* planes, respectively. From left to right: FTEs during all, southward, and northward IMF orientations, respectively. T96 model [*Tsyganenko*, 1995] magnetic field lines are shown in each panel as the background for reference.

magnitude shows a strong dependence on MLAT. The larger the absolute FTE magnetic latitude, the larger FTE B_N peak-peak magnitude tends to be. The B_N peak-peak magnitude dependence on Earth dipole tilt is more complex, with no major variation for negative Earth dipole tilt, a peak when Earth dipole tilt is close to zero, and decreasing B_N peak-peak magnitude with increasing positive Earth dipole tilt.

[18] Figure 6, from left to right, shows the FTE separation time dependence on MLT, MLAT, and Earth dipole tilt, all without thresholds. Only FTE separation times less than 20 min are used in this plot, assuming that intervals larger than 20 min are not part of the same reconnection sequence [*Neudegg et al.*, 2000]. The MLT, MLAT, and Earth dipole tilt values for each FTE separation time are the averages of their corresponding values for the two FTEs concerned. The thick horizontal bars are the medians of FTE separation time for the MLT, MLAT, and Earth dipole tilt ranges that they span. The thin horizontal bars are the standard errors of the median values that they correspond. From the figure, we see a general increase of FTE separation time with increasing MLT. FTE separation time peaks at around zero Earth dipole tilt and it generally decreases with increasing absolute Earth dipole tilt. There is no clear dependence of FTE separation time on MLAT.

[19] The left panel of Figure 7 shows the FTE B_N peak-peak magnitude dependence on FTE separation time. The B_N peak-peak magnitude for each FTE separation time is

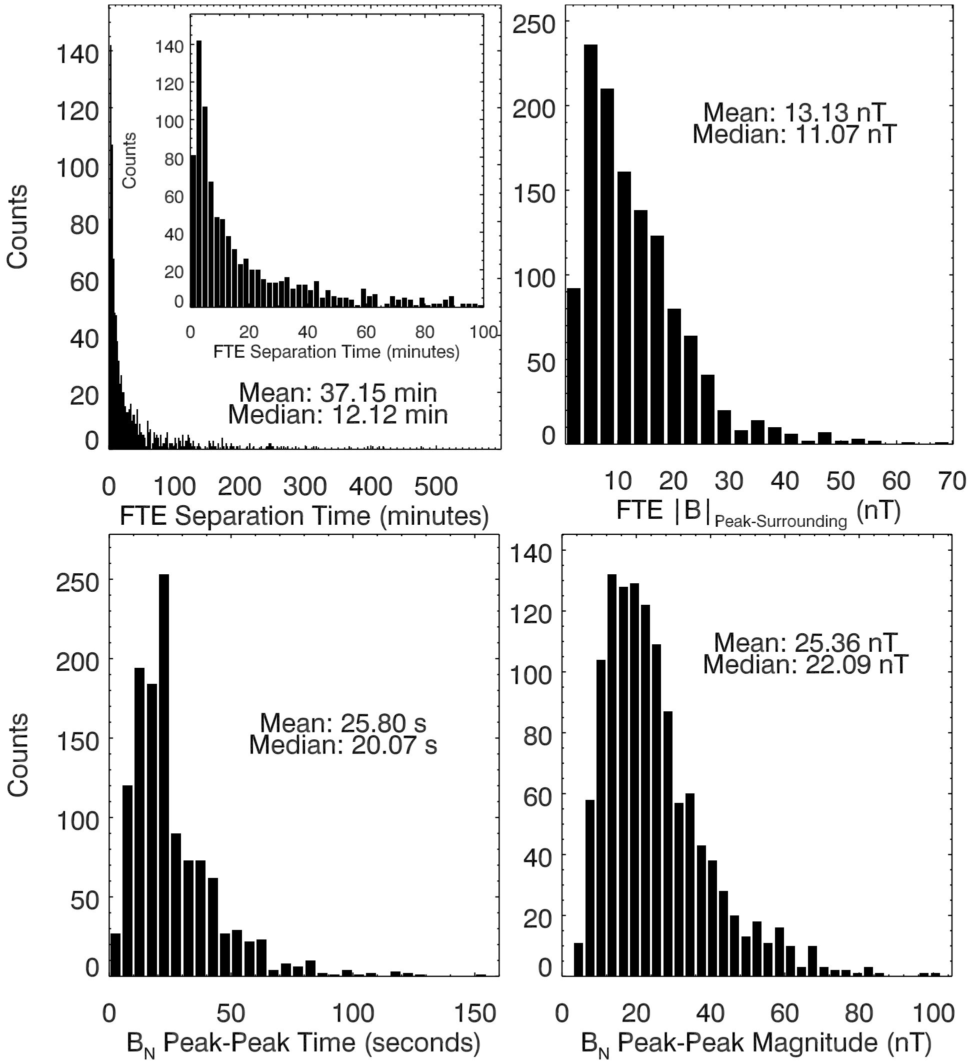

Figure 4. The FTE separation time distribution, FTE $|\mathbf{B}|_{peak-surrounding}$ distribution, FTE B_N peak-peak time distribution, and FTE B_N peak-peak magnitude distribution, all with no thresholds. Note here that each FTE separation time in the upper left panel is calculated between two contiguous FTEs without requiring that they correspond to the same Cluster magnetopause crossing.

the average of the corresponding values of the two FTEs for the separation time. The right panel of the figure shows the FTE B_N peak-peak magnitude dependence on FTE B_N peak-peak time. In both panels, the thick horizontal bars are the medians of FTE B_N peak-peak magnitude in the horizontal ranges that they span, the thin horizontal bars are the standard errors of the median values that they correspond. In the figure, FTE B_N peak-peak magnitude generally increases with increasing FTE separation time. We see no strong dependence of B_N peak-peak magnitude on FTE B_N peak-peak time.

5. Discussion

[20] As pointed out by Wang et al. (submitted manuscript, 2005), among the 1222 Cluster FTEs in this study without quantitative FTE identification thresholds, 57% correspond to southward IMF and 43% correspond to northward IMF,

Table 1. Some FTE Statistical Parameters for Different Thresholds

	IMF		Mean	Mean	Mean	Inside	Outside
Threshold	$B_z < 0$	$B_z > 0$	$T_{B_{N,peak-peak}}$	$\lvert B_{N,peak-peak}\rvert$	$\lvert\mathbf{B}\rvert_{peak-surrounding}$	MP	MP
0[a]	57%	43%	25.8 s	25.4 nT	13.1 nT	73%	27%
1[b]	61%	39%	26.4 s	32.0 nT	19.3 nT	72%	28%
2[c]	65%	35%	26.2 s	38.8 nT	25.4 nT	71%	29%

[a]No thresholds.
[b]$|B_{N,peak-peak}| \geq 10$ nT and $|\mathbf{B}|_{peak-surrounding} \geq 10$ nT.
[c]$|B_{N,peak-peak}| \geq 17$ nT and $|\mathbf{B}|_{peak-surrounding} \geq 17$ nT.

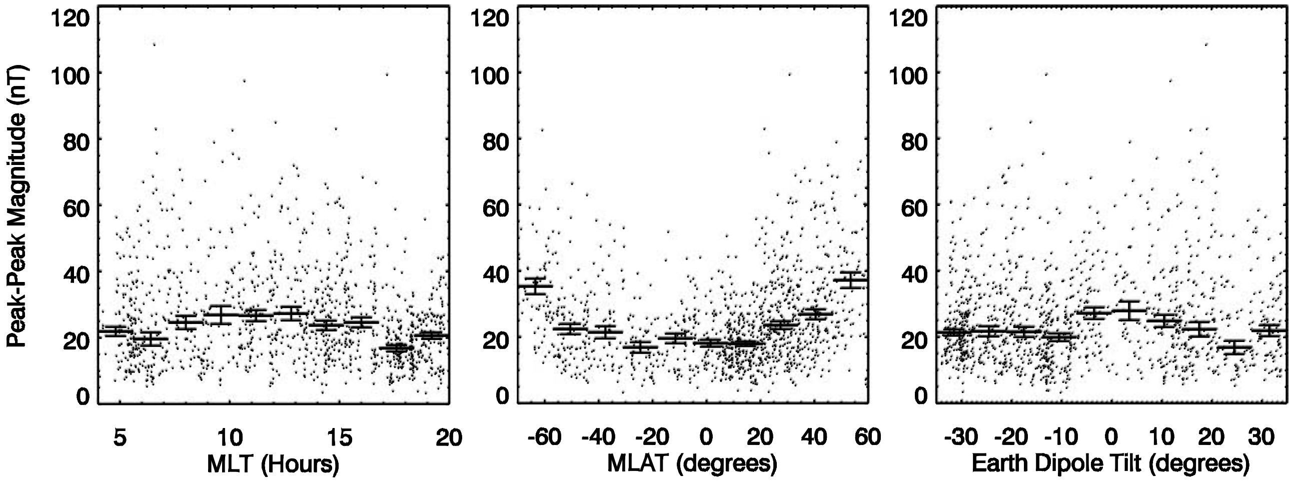

Figure 5. From left to right: The FTE B_N peak-peak magnitude dependence on MLT, MLAT, and Earth dipole tilt, all without quantitative FTE identification thresholds. The thick horizontal bars are the medians of FTE B_N peak-peak magnitude for the horizontal ranges that they span. The thin horizontal bars are the standard errors of the median values that they correspond.

and such a large proportion of northward IMF FTEs is possibly caused by high-latitude reconnection [*Wild et al.*, 2001; *Vontrat-Reberac et al.*, 2003]. Supporting evidence for the above conclusion is shown in the right panels of Figure 3 where there are a significant number of high-latitude FTEs during northward IMF. Also in the right panels of the same figure there are a large number of low-latitude flank FTEs during northward IMF. *Kawano and Russell* [1997a] provided four possible explanations for similar cases during northward IMF in their ISEE FTE study: (1) a possible negative B_L component at the postterminator magnetopause causing local reconnection; (2) tilted equatorial reconnection at the postterminator magnetopause; (3) polar cusp reconnection; and (4) random reconnection around the subsolar magnetopause (please refer to their paper for more detailed discussion). *Kawano and Russell* [1997b] further evaluated these possible explanations and found that explanations 2 and 3 were supported by ISEE FTE observations.

[21] The FTE separation times from all our Cluster FTEs without quantitative identification thresholds have an average of 37.15 min (median: 12.12 min), which is significantly larger than the previous results. If we follow *Neudegg et al.*'s [2000] assumption to remove larger than 20 min intervals, an average FTE separation time of 7.09 min (median: 5.62 min) is obtained. These mean and median FTE separation times are at the lower ends of the previous results. A possible explanation for our smaller FTE separation times is that there is an additional source of FTEs from high-latitude reconnection than the low-latitude observations. *Kawano and Russell* [1996] found from their ISEE

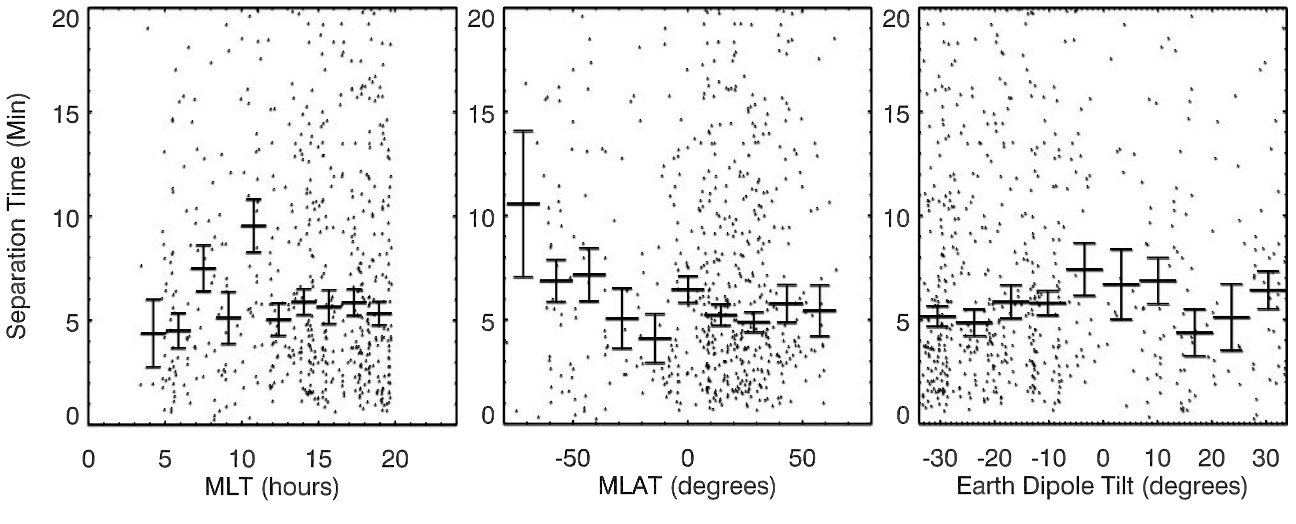

Figure 6. From left to right: The FTE separation time dependence on MLT, MLAT, and Earth dipole tilt, all without thresholds. Only FTEs with separation times less than 20 min are used in this plot. The MLT, MLAT, and Earth dipole tilt values for each FTE separation time are the averages of their corresponding values of the two FTEs for the separation time. The thick horizontal bars are the medians of FTE separation time for the horizontal ranges that they span. The thin horizontal bars are the standard errors of the median values that they correspond.

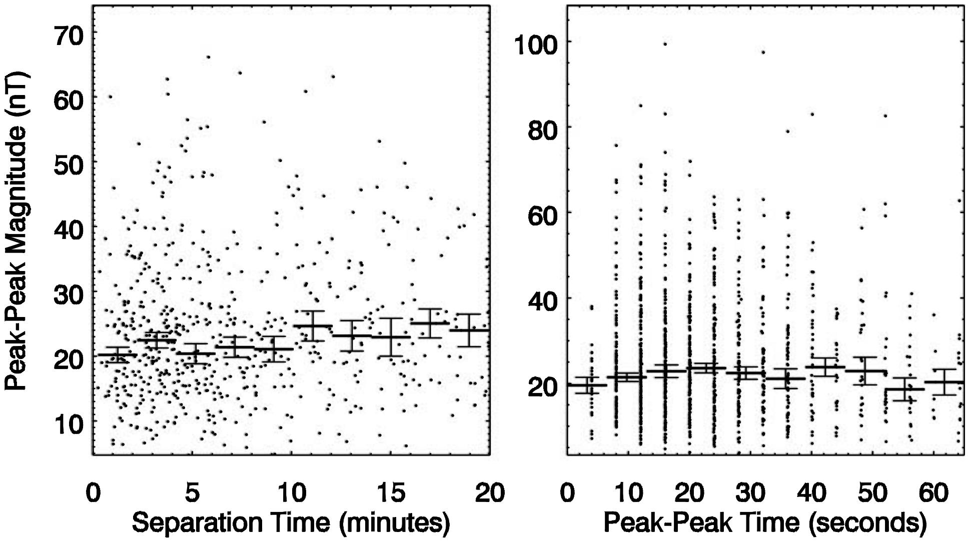

Figure 7. (left) The FTE B_N peak-peak magnitude dependence on FTE separation time for FTEs without thresholds. The B_N peak-peak magnitude for each FTE separation time is the average of B_N peak-peak magnitude of the two FTEs for the separation time. (right) The FTE B_N peak-peak magnitude dependence on FTE B_N peak-peak time. The stripes are caused by the Cluster data sampling rate of 4 s. The thick horizontal bars are the medians of FTE B_N peak-peak magnitude for the horizontal ranges that they span. The thin horizontal bars are the standard errors of the median values that they correspond.

FTE study that the occurrence rate of FTEs tends to increase with decreasing distance from the magnetopause. Thus it is also possible that Cluster skims along the magnetopause much longer near the low-latitude magnetopause flanks than those low-latitude satellites used in previous FTE studies, thus allowing Cluster to see more subsequent FTEs, which leads to shorter FTE separation time.

[22] We obtain a mean B_N peak-peak magnitude of 25.36 nT (median: 22.09 nT) and an average FTE B_N peak-peak time of 25.79 s (median: 20.07 s). Our median B_N peak-peak time falls within 36 s obtained by *Kawano and Russell* [1996] and 3 min obtained by *Sanny et al.* [1996]. The low B_N peak-peak duration identification criteria used in these two previous studies definitely contribute to their larger B_N peak-peak duration. Our median B_N peak-peak magnitude is significantly larger than that from *Kawano and Russell* [1996], which is surprising, especially since we did not use a lower threshold for B_N peak-peak magnitude during FTE identification. Since *Kawano and Russell*'s [1996] ISEE database also includes low-latitude magnetopause flank FTEs, this large difference may imply that high-latitude FTEs have systematically larger magnitude than low-latitude FTEs. In support of this, the middle panel of Figure 5 shows that FTE B_N peak-peak magnitude increases with increasing absolute MLAT. It is also indirectly supported by FTE B_N peak-peak magnitude dependence on MLT in the left panel of the same figure. There is a weak FTE B_N peak-peak magnitude peak close to the magnetic local noon (MLT = 12) where FTEs are observed at the high-latitude magnetopause (see Figure 3). While FTE B_N peak-peak magnitude is smaller farther away from the magnetic local noon at the magnetopause flanks where there are many low-latitude FTEs. This systematic trend of increased FTE B_N peak-peak magnitude with increasing MLAT might be caused by the stronger sheath fields draped over the FTEs when the FTEs propagate from low-latitude magnetopause to the high-latitude magnetopause.

[23] In Table 1, ~72% of the Cluster FTEs are observed outside of the magnetopause crossings for different thresholds, and this percentage does not change much for both low- and high-latitude FTEs. This is consistent with the midlatitude FTE study results of *Neudegg et al.* [2000]. The greater number of FTEs observed outside than inside of the magnetopause at the midlatitude and high-latitude magnetopause, as well as the low-latitude flanks, than the low-latitude subsolar magnetopause [*Rijnbeek et al.*, 1984; *Berchem and Russell*, 1984; *Kawano and Russell*, 1996] might imply that there is a significant motion of the FTEs, originated at the low-latitude dayside magnetopause, from inside the magnetopause to the magnetosheath when they propagate away from their origin. If this is true, such motion should be caused by the interaction between the FTEs and surrounding plasma and field in the complex magnetopause and magnetosheath environment. More studies, especially numerical studies, are needed to explain what processes cause such FTE evolution. On the other hand, it is also possible that FTEs generated on the magnetopause away from the low-latitude dayside magnetopause are more likely to extend more outside of the magnetopause than FTEs generated at low-latitude dayside magnetopause.

[24] Wang et al. (submitted manuscript, 2005) found from their Cluster FTE study that the normalized FTE MLAT dependence without thresholds has a peak near the magnetic equator and it decreases farther away from it. They believed that this result is likely caused by the orbital bias of Cluster because, for a given high-latitude magnetopause crossing at the magnetopause flank, Cluster spends a significant amount of time close to the low-latitude magnetopause which allows more chance to see FTEs. For the case with Threshold 2, a much more flattened normalized FTE MLAT dependence is obtained. They believed that it is likely the result of the strong

constraints which remove low-latitude flank FTEs. Supporting evidence for the above assertion is shown in the middle panel of Figure 5 which shows that FTE B_N peak-peak magnitude increases with increasing absolute MLAT. Thus when we use thresholds with larger $|B_{N,peak-peak}|$ lower limit, we are more likely to remove low-latitude FTEs, which helps cancel the Cluster orbital bias for FTE MLAT dependence.

[25] We obtain an average FTE separation time consistent with previous results by assuming that FTEs with intervals larger than 20 min are not part of the same reconnection sequence. In Figure 6 we show the FTE separation time-dependence on MLT, MLAT, and Earth dipole tilt, also neglecting separation times larger than 20 min. From the figure, we see a slight increase of FTE separation time with increasing MLT. FTE separation time peaks at around zero Earth dipole tilt and it generally decreases with increasing absolute Earth dipole tilt. These results confirm *Russell et al.*'s [1997] conclusion that FTE generation rate can be controlled by some geophysical parameters. In contrast, there is no clear dependence of FTE separation time on MLAT. We leave the possibility of solar wind control of FTE generation and periodicity for a later study.

[26] In Table 1 we show that some FTE statistical parameters, including mean B_N peak-peak time, and the percentage of FTEs inside/outside of the magnetopause, only change slightly for different thresholds. This is consistent with the assertion by *Southwood et al.* [1986] and the results reported by Wang et al. (submitted manuscript, 2005) that different criteria used in the FTE studies should not influence the results in a significant way. On the other hand, by not using quantitative FTE identification thresholds, we can avoid numerical errors introduced by arbitrary thresholds during FTE identification, thus allowing more accurate calculations of some FTE statistical parameters, for example, FTE B_N peak-peak time discussed earlier in this section. More importantly, comparing statistical results with different thresholds can help obtain useful information about FTEs. For example, Table 1 shows the numbers of FTEs for southward and northward IMF for different thresholds. By increasing the threshold, larger proportion of FTEs are seen during southward IMF: 57% for Threshold 0, 61% for Threshold 1, and 65% for Threshold 2. Thus FTEs during southward IMF should have larger B_N peak-peak magnitude than FTEs during northward IMF (Wang et al., submitted manuscript, 2005). This is directly confirmed by the mean B_N peak-peak magnitude for FTEs during southward IMF (26.30 nT) and northward IMF (24.09 nT). Also, the mean B_N peak-peak time in Table 1 changes very little for Thresholds 0, 1, and 2, from which we can infer that there should be no strong correlation between FTE B_N peak-peak time and B_N peak-peak magnitude (and $|\mathbf{B}|_{peak-surrounding}$). This is confirmed by a direct comparison between B_N peak-peak magnitude and B_N peak-peak time in Figure 7.

6. Summary

[27] From this large-scale Cluster high-latitude magnetopause and low-latitude flank FTE statistical study, we reach the following conclusions:

[28] 1. Cluster FTEs are observed at both the high-latitude magnetopause and low-latitude flanks for both southward and northward IMF.

[29] 2. Among the 1222 Cluster FTEs, 36%, 20%, 14%, and 30% are seen by one, two, three, and four Cluster satellites, respectively.

[30] 3. There are 73% (27%) of the Cluster FTEs observed outside (inside) of the magnetopause, which is significantly different from the results form low-latitude FTE studies. This might imply that there is a significant motion of the FTEs, originated at the low-latitude dayside magnetopause, from inside the magnetopause to the magnetosheath when they propagate to the midlatitude and high-latitude magnetopause, and the low-latitude magnetopause flanks.

[31] 4. We obtain an average FTE separation time of 7.09 min, which is at the lower end of the previous results. This might be caused by additional source of FTEs at the high-latitude magnetopause or the Cluster orbital effect of skimming longer along the magnetopause flanks.

[32] 5. The mean B_N peak-peak magnitude of Cluster FTEs is significantly larger than that from low-latitude FTE studies. Further, FTE B_N peak-peak magnitude clearly increases with increasing absolute MLAT. This systematic trend might be caused by the stronger sheath fields draped over the FTEs when the FTEs propagate from low-latitude magnetopause to the high-latitude magnetopause. There is a weaker dependence of FTE B_N peak-peak magnitude on MLT with a peak near 12 MLT and the magnitude generally decreases farther away from the magnetic local noon. The B_N peak-peak magnitude dependence on Earth dipole tilt is more complex with a peak at around zero Earth dipole tilt.

[33] 6. FTE periodic behavior is found to be controlled by MLT, with a slight increase of FTE separation time for increasing MLT, and by Earth dipole tilt, with a peak FTE separation time at around zero Earth dipole tilt. There is no clear dependence of FTE separation time on MLAT.

[34] 7. There is a weak increase of FTE B_N peak-peak magnitude with increasing FTE separation time and we see no clear dependence of B_N peak-peak magnitude on FTE B_N peak-peak time.

[35] 8. We further confirm that FTE statistic results do not change in a significant way by using different FTE criteria. When no thresholds are used, more accurate calculations of some FTE statistical parameters, including mean B_N peak-peak time, can be obtained. Further, comparing results with different thresholds can help obtain useful information about FTEs, e.g., southward IMF should correspond to FTEs with larger peak-peak magnitude, and there should be no strong correlation between FTE B_N peak-peak time and B_N peak-peak magnitude, which are confirmed through other direct methods.

[36] **Acknowledgments.** This research was carried out under the auspices of the US Department of Energy under NASA OFSS 10,205, the Cluster Guest Investigator Program. The work at UCLA was supported by NSF under grant ATM 04-02213. We thank Cluster FGM and CIS teams and ACE SWEPAM and MFI teams for providing the data. YLW would like to thank M. F. Thomsen for helpful discussions and the reviewers for helpful comments.

[37] Lou-Chuang Lee thanks Zhi-wei Ma and David Sibeck for their assistance in evaluating this paper.

References

Balogh, A., et al. (1997), The Cluster magnetic field investigation, *Space Sci. Rev.*, *79*, 65–91.

Berchem, J., and C. T. Russell (1984), Flux transfer events on the magnetopause: Spatial distribution and controlling factors, *J. Geophys. Res.*, *89*, 6689–6703.

Bosqued, J. M., et al. (2001), Cluster observations of the high-latitude magnetopause and cusp: Initial results from the CIS ion instruments, *Ann. Geophys.*, *19*, 1545–1566.
Daly, P. W., D. J. Williams, C. T. Russell, and E. Keppler (1981), Particle signature of magnetic flux transfer events at the magnetopause, *J. Geophys. Res.*, *86*, 1628–1632.
Elphic, R. C. (1990), Observations of flux transfer events: Are FTE's flux ropes, islands or surface waves?, in *Physics of Magnetic Flux Ropes*, *Geophys. Monogr. Ser.*, vol. 58, edited by C. T. Russell, E. R. Priest, and L. C. Lee, pp. 455–471, AGU, Washington, D. C.
Haerendel, G., G. Paschmann, N. Sckopke, H. Rosenbauer, and P. C. Hedgecock (1978), The frontside boundary layer of the magnetosphere and the problem of reconnection, *J. Geophys. Res.*, *83*, 3195–3216.
Kawano, H., and C. T. Russell (1996), Survey of flux transfer events observed with the ISEE 1 spacecraft: Rotational polarity and the source region, *J. Geophys. Res.*, *101*, 27,299–27,308.
Kawano, H., and C. T. Russell (1997a), Survey of flux transfer events observed with the ISEE 1 spacecraft: Dependence on the interplanetary magnetic field, *J. Geophys. Res.*, *102*, 11,307–11,313.
Kawano, H., and C. T. Russell (1997b), Cause of post terminator flux transfer events, *J. Geophys. Res.*, *102*, 27,029–27,038.
Kawano, H., S. Kokubun, and K. Takahashi (1992), Survey of transient magnetic field events in the dayside magnetosphere, *J. Geophys. Res.*, *97*, 10,677–10,692.
Kuo, H., C. T. Russell, and G. Le (1995), Statistical studies of flux transfer events, *J. Geophys. Res.*, *100*, 3513–3519.
Le, G., C. T. Russell, and H. Kuo (1993), Flux transfer events: Spontaneous or driven?, *Geophys. Res. Lett.*, *20*, 791–794.
Lee, L. C., and Z. F. Fu (1985), A theory of magnetic flux transfer at the Earth's magnetopause, *Geophys. Res. Lett.*, *12*, 105–108.
Liu, Z. X., Z. W. Zhu, F. Li, and Z. Y. Pu (1992), Topology and signatures of a model for flux transfer events based on vortex-induced reconnection, *J. Geophys. Res.*, *97*, 19,351–19,361.
Lockwood, M., and M. N. Wild (1993), On the quasi-periodic nature of magnetopause flux transfer events, *J. Geophys. Res.*, *98*, 5935–5940.
McComas, D. J., S. J. Bame, P. Barker, W. C. Feldman, J. L. Phillips, P. Riley, and J. W. Griffee (1998), Solar Wind Electron Proton Alpha Monitor (SWEPAM) for the Advanced Composition Explorer, *Space Sci. Rev.*, *86*, 563–612.
Neudegg, D. A., et al. (2000), A survey of magnetopause FTEs and associated flow bursts in the polar ionosphere, *Ann. Geophys.*, *18*, 416–435.
Owen, C. J., et al. (2001), Cluster PEACE observations of electrons during magnetospheric flux transfer events, *Ann. Geophys.*, *19*, 1509–1522.
Paschmann, G., G. Haerendel, I. Papamastorakis, N. Sckopke, S. J. Bame, J. T. Gosling, and C. T. Russell (1982), Plasma and magnetic field characteristics of magnetic flux transfer events, *J. Geophys. Res.*, *87*, 2159–2168.
Raeder, J. (2005), Flux transfer events: Generation mechanism for nearly southward IMF, *Ann. Geophys.*, in press.
Rème, H., et al. (2001), First multispacecraft ion measurements in and near the Earth's magnetosphere with the identical Cluster ion spectrometry (CIS) experiment, *Ann. Geophys.*, *19*, 1303–1354.
Rijnbeek, R. P., S. W. H. Cowley, D. J. Southwood, and C. T. Russell (1984), A survey of dayside flux transfer events observed by ISEE 1 and 2 magnetometers, *J. Geophys. Res.*, *89*, 786–800.
Russell, C. T., and R. C. Elphic (1978), Initial ISEE magnetometer results: Magnetopause observations, *Space Sci. Rev.*, *22*, 681–715.
Russell, C. T., and R. C. Elphic (1979), ISEE observation of flux events at the dayside magnetopause, *Geophys. Res. Lett.*, *6*, 33–36.
Russell, C. T., G. Le, H. Kawano, S. M. Petrinec, and T. L. Zhang (1997), Intrinsic time scale for reconnection on the dayside magnetopause, *Adv. Space Res.*, *19*, 1913–1917.
Saflekos, N. A., J. L. Burch, M. Sugiura, D. A. Gurnett, and J. L. Horwitz (1990), Observations of reconnected flux tubes within the midaltitude cusp, *J. Geophys. Res.*, *95*, 8037–8055.
Sanny, J., D. G. Sibeck, C. C. Venturini, and C. T. Russell (1996), A statistical study of transient events in the outer dayside magnetosphere, *J. Geophys. Res.*, *101*, 4939–4952.
Sanny, J., C. Beck, and D. G. Sibeck (1998), A statistical study of the magnetic signatures of FTEs near the dayside magnetopause, *J. Geophys. Res.*, *103*, 4683–4692.
Scholer, M. (1988), Magnetic flux transfer at the magnetopause based on single X line bursty reconnection, *Geophys. Res. Lett.*, *15*, 291–294.
Shue, J. H., et al. (1998), Magnetopause location under extreme solar wind conditions, *J. Geophys. Res.*, *103*, 17,691–17,700.
Sibeck, D. G. (1990), A model for the transient magnetospheric response to sudden solar wind dynamic pressure variations, *J. Geophys. Res.*, *95*, 3755–3771.
Smith, C. W., J. N. F. L'Heureux, M. H. Acuña, L. F. Burlaga, and J. Scheifele (1998), The ACE Magnetic Fields Experiment, *Space Sci. Rev.*, *86*, 613–632.
Sonnerup, B. U. Ö., H. Hasegawa, and G. Paschmann (2004), Anatomy of a flux transfer event seen by Cluster, *Geophys. Res. Lett.*, *31*, L11803, doi:10.1029/2004GL020134.
Southwood, D. J., M. A. Saunders, M. W. Dunlop, W. A. C. Mierjedrzejowicz, and R. P. Rijnbeek (1986), A survey of flux transfer events recorded by the UKS spacecraft magnetometer, *Planet. Space Sci.*, *34*, 1349–1359.
Suvorova, A. V., A. V. Dmitriev, and S. N. Kuznetsov (1999), Dayside magnetopause models, *Radiat. Meas.*, *30*, 687–692.
Thompson, S. M., M. G. Kivelson, K. K. Khurana, A. Balogh, H. Réme, A. N. Fazakerley, and L. M. Kistler (2004), Cluster observations of quasi-periodic impulsive signatures in the dayside northern lobe: High-latitude flux transfer events?, *J. Geophys. Res.*, *109*, A02213, doi:10.1029/2003JA010138.
Tsyganenko, N. A. (1995), Modeling the Earth's magnetospheric magnetic field confined within a realistic magnetopause, *J. Geophys. Res.*, *100*, 5599–5612.
Vontrat-Reberac, A., et al. (2003), Cluster observations of the high-altitude cusp for northward interplanetary magnetic field: A case study, *J. Geophys. Res.*, *108*(A9), 1346, doi:10.1029/2002JA009717.
Wild, J. A., et al. (2001), First simultaneous observations of flux transfer events at the high-latitude magnetopause by the Cluster spacecraft and pulsed radar signatures in the conjugate ionosphere by the CUTLASS and EISCAT radars, *Ann. Geophys.*, *19*, 1491–1508.
Zong, Q. G., T. A. Fritz, H. Spence, M. Dunlop, Z. Y. Pu, A. Korth, P. W. Daly, A. Balogh, and H. Réme (2003), Bursty energetic electrons confined in flux ropes in the cusp region, *Planet. Space Sci.*, *51*, 821–830.

J. Birn, R. C. Elphic, R. H. Friedel, B. Lavraud, and Y. L. Wang, Space Science and Applications, Los Alamos National Laboratory, P.O. Box 1663, MS D466, Los Alamos, NM 87545, USA. (jbirn@lanl.gov; relphic@lanl.gov; rfriedel@lanl.gov; lavraud@lanl.gov; ywang@lanl.gov)

H. Kawano, Department of Earth and Planetary Sciences, Kyushu University, 6-10-1 Hakozaki, Higashi-ku, Fukuoka City, Fukuoka 812-8581, Japan. (hkawano@geo.kyushu-u.ac.jp)

J. Raeder, Space Science Center, University of New Hampshire, 245G Morse Hall, 39 College Road, Durham, NH 03824, USA. (j.raeder@unh.edu)

C. T. Russell, Institute of Geophysics and Planetary Physics, University of California, Los Angeles, 405 Hilgard Avenue, Los Angeles, CA 90095-1567, USA. (ctrussel@igpp.ucla.edu)

M. G. G. T. Taylor, Mullard Space Science Laboratory, University College London, Holmbury St. Mary, Dorking, Surrey RH5 6NT, UK. (mggt@mssl.ucl.ac.uk)

H. Zhang and Q.-G. Zong, Center for Space Physics, Boston University, 725 Commonwealth Avenue, Boston, MA 02215, USA. (zhang@bu.edu; zong@bu.edu)

X. X. Zhang, Center for Space Science and Applied Research, P.O. Box 8701, Beijing 100080, China. (xxzhang@spaceweather.ac.cn)